ISSN 2436-5173 (Online)

Metallomics Research

Vol. 4/No. 1
February 2024

Japan Society for
Biomedical Research on Trace Elements

Metallomics Research

Vol. 4 / No. 1
February 2024
ISSN 2436-5173 (Online)

Japan Society for
Biomedical Research on Trace Elements

Index

Editorial Office

Seishinsha, co. Ltd.,
Japan society for Biomedical Research on Trace Elements
2-8-13 Fukashi, Matsumoto-shi, Nagano 390-0815, Japan
Tel: +81-263-32-2301 Fax: +81-263-36-4691 Editorial Office: brte-post@seisin.cc
URL: https://www.brte.org/ https://metallomicsresearch.brte.org/

Regular Article https://metallomicsresearch.brte.org

Impact of *hepcidin* mRNA expression in the liver of patients with chronic hepatitis C or liver cirrhosis

Mitsuhiko Moriyama[1,2], Hitomi Nakamura[1], Masahiro Ogawa[1], Toshikatu Shibata[1], Kazumichi Kuroda[1]

[1] Division of Gastroenterology and Hepatology, Department of Medicine, Nihon University School of Medicine,
[2] Sashiogi Recuperation Hospital.

Abstract

Background: We aimed to investigate the correlation between *hepcidin* mRNA expression and the pathophysiology of the liver or the long-term prognosis in patients with chronic hepatitis C (CHC) or liver cirrhosis (LC).

Methods: A total of 82 patients with CHC or LC who underwent liver biopsy were included in this study. *Hepcidin* mRNA expression was detected in the frozen liver tissues obtained from patients with CHC or LC who underwent liver biopsy. *Hepcidin* mRNA expression in frozen liver tissues was assessed using real-time quantitative polymerase chain reaction. We previously reported that the extent of proliferation of atypical hepatocytes (POAH) within the six-cell lesion of irregular regeneration (IR) of hepatocytes is a significant histological finding associated with the development of hepatocellular carcinoma (HCC) from CHC or LC. Therefore, we investigated the association between *hepcidin* mRNA expression and disease severity, pathological findings such as the extent of POAH, and the incidence of HCC development from CHC and LC. Furthermore, we compared *hepcidin* mRNA expression with serum cytokine and chemokine levels using a Bio-plex suspension array system (Bio-Rad Laboratories, CA, USA).

Results: *Hepcidin* mRNA expression was associated with serum ferritin concentration (p=0.009) and unsaturated iron-binding capacity (P=0.0003) in the serological parameters, but no association was found with histological parameters. The cumulative incidence of HCC development was significantly higher in the low *hepcidin* mRNA expression group than in the high *hepcidin* mRNA expression group (p=0.003). Additionally, patients with lower *hepcidin* mRNA levels tended to exhibit more extensive POAH (p=0.0089). *Hepcidin* mRNA expression was also significantly associated with apoptosis-related and anti-inflammatory cytokines/chemokines.

Conclusions: Low *hepcidin* mRNA expression may be a risk factor for carcinogenesis in patients with CHC or LC.

*Correspondence:
Mitsuhiko Moriyama
Sashiogi Recuperation Hospital,
1348-1 Hourai, nishi-ku, Saitama city, Saitama prefecture
331-0074, Japan.
Tel ; +81 48 623 1102 Fax ; +81 48 623 7474
e-mail ; moriyama.mitsuhiko@nihon-u.ac.jp

Received: November 15, 2023
Accepted: January 22, 2024
Released online: February 15, 2024

Keywords:
hepcidin, Real-time quantitative RNA (RT-qPCR), hepatocellular carcinoma (HCC), chronic hepatitis C (CHC), liver cirrhosis (LC), Bio-plex suspension array, proliferation of atypical hepatocytes (POAH)

Competing interests:
Mitsuhiko Moriyama; Towa Pharmaceutical Co., Ltd. The other authors have no conflict of interest to declare.

Introduction

Although iron is an essential element for the human body,

 DOI https://doi.org/10.11299/metallomicsresearch.MR202310

excessive amounts of free iron (Fe^{2+}) can be toxic. Excess iron can catalyze the formation of free radicals, which may lead to various cellular disorders. Therefore, the human body tightly regulates intracellular iron levels and the peptide hormone hepcidin, plays a crucial role by binding to the iron export transporter ferroportin (FPN) [1]. Elevated serum iron levels results in rapid inhibition of iron transport [2] and the degradation of cell-surface FPN [3-6], which in turn inhibits FPN-mediated dietary iron absorption and iron release from intracellular iron stores. As a result, dysregulation of hepcidin or FPN expression can lead to iron disorders in humans.

Hepcidin expression in the liver is a complex process that is regulated by various factors including iron overload and inflammation which increase hepcidin expression, whereas hypoxia and erythropoiesis decrease expression [7-9]. In patients with chronic viral liver disease, hepcidin expression has also been reported to influence hepatic morbidity and pathophysiology [10-12]. We hypothesized that hepatic hepcidin expression is associated with liver morbidity in nonalcoholic steatohepatitis (NASH). Therefore, we previously investigated hepatic hepcidin expression using a rat model of NASH development [13], and found that *hepcidin* mRNA expression decreases with the progression of NASH, which led us to speculate that hepcidin may be linked to the pathogenesis of NASH.

According to reports, hepcidin is involved in the progression of steatohepatitis, including NASH and metabolic dysfunction-associated steatotic liver disease [14-16]. Impaired iron translocation from the hepatocytes and Kupffer cells is the primary cause of iron accumulation in nonalcoholic fatty liver disease. Impaired iron transport is associated with inflammation and metabolic abnormalities that affect iron regulators, such as hepcidin, ferroportin, transferrin receptors, ferritin, and copper [17,18].

Furthermore, our previous research revealed that phlebotomy in patients with chronic hepatitis C (CHC) or liver cirrhosis (LC) can reduce transaminase levels and the cumulative incidence of hepatocellular carcinoma (HCC) development in patients with CHC and LC [19]. Therefore, we hypothesized iron overload is associated with the progression of CHC or LC and the development of HCC from CHC or LC. We have also reported that intrahepatic iron concentration affects the pathogenesis of chronic hepatitis [20]. Herein, we hypothesized that liver iron overload and *hepcidin* mRNA expression in the liver are linked to the severity of liver disease and the development of HCC.

Regarding histological factors that are associated with carcinogenesis in liver sections, the degree of irregular regeneration (IR) of hepatocytes was reported by Uchida et. al. [21-23]. The theory of the IR of hepatocytes was proposed by Peters [24] and Uchida [21-23]. The IR of hepatocytes in lobules is a general term encompassing anisocytosis of hepatocytes, map-like distribution, nodular arrangement of parenchyma, oncocytic change of hepatocytes, proliferation of atypical hepatocytes, and bulging of hepatocytes.

Recently, we defined the grade according to the IR of each group of hepatocytes, and examined the correlation between the IR grade in hepatocytes and the occurrence of HCC in chronic hepatitis C or cirrhosis [25]. The analysis revealed that the extent of proliferation of atypical hepatocytes (POAH) was a strong histological risk factor for HCC development. Atypical hepatocytes are generally characterized by smaller cells with a higher nucleoplasmic (N/C) ratio, nuclei that show mild size disparity, cytoplasm with enhanced eosinophilia, a clear distinction between atypical and normal hepatocytes, and the absence of fat droplets [26,27]. It has been reported that the degree of proliferation of atypical hepatocytes (POAH) within the six-cell lesion of IR of hepatocytes is a significant histological finding associated with the development of HCC from CHC or LC [19,23,25]. Therefore, we hypothesized that the level of expression of *hepcidin* mRNA in chronic hepatitis represents a highly carcinogenic state of the liver. Hence, we investigated the relationship between liver histology, including the extent of POAH and *hepcidin* mRNA expression.

We then examined the cytokines/chemokines that regulate *hepcidin* mRNA expression using a multiplex cytokine assay to detect serum cytokine/chemokine concentrations. Based on these studies, we investigated whether *hepcidin* mRNA expression levels are associated with the progression of liver disease and the development of HCC from CHC and LC. The expression of *hepcidin* mRNA was quantified using the formula: $\Delta Ct = Ct_{\text{for hepcidin gene test}} - Ct_{\text{glyceraldehyde–3–phosphate dehydrogenase (GAPDH) test}}$.

Materials and methods

Participants

The study population comprised 82 hepatitis C virus (HCV) RNA-positive patients who underwent liver biopsy at Nihon University Itabashi Hospital between January 1, 2001 and December 25, 2008. These patients were selected based on the feasibility of using cryopreserved liver biopsy specimens. The participants were HCV RNA-positive patients with CHC or LC

who consented to long-term prognostic evaluation and participation in the study. The clinical characteristics of the patients are presented in **Table 1**. The enrolled patients were assigned an F stage according to the INUYAMA and Demet classification, with F0 to F3 designated as CHC, and F4 as LC [28,29].

Of the 82 patients, 49 whose cytokine and chemokine levels were previously measured [30] were analyzed for correlations between *hepcidin* mRNA expression and cytokine and chemokine concentrations. These patients comprised 27 males and 22 females and were classified into four F stages as follows: F1 (n=21), F2 (n=13), F3 (n=6), and F4 (n=9).

Table 1. | Clinical profiles of participants (n=82)

	Chronic hepatitis (F0 to F3)	Liver cirrhosis (F4)
number	63	19
observation periods (yrs)	8.8 (0.1-14.1)	6.3 (0.4-12.4)
age (yrs)	54.0 (23.5-73.7)	59.8 (44.8-74.1)
gender (males)	35 (54.7%)	9 (47.4%)
AST (U/L)	44.5 (15-183)	74.0 (40-129)
ALT (U/L)	55.5 (10-328)	79.0 (45-138)
r-GT (U/L)	39.0 (10-303)	50.0 (24-128)
ALP (U/L)	246.0 (111-624)	331.0 (163-1370)
total bilirubin (mg/dl)	0.60 (0.25-1.47)	0.70 (0.40-1.38)
platelet counts(x10^4)	18.2 (7.3-38.1)	11.9 (9.6-22.8)
total protein (g/dl)	7.2 (6.1-8.6)	7.3 (6.7-8.6)
albumin (g/dl)	4.0 (3.4-4.7)	3.6 (3.1-6.9)
prothrombin time (%)	96 (69-100)	92 (79-100)
BTR	5.94 (4.06-12.20)	5.29 (2.82-8.00)
BCAA	489 (352-677)	477 (259-825)
tyrosine	83 (40-126)	92 (63-151)
ammonia (μg/dl)		
ICGR15 (%)	7.0 (1.4-21.2)	14.0 (2.1-71.1)
zinc concetration (μg/dl)	74 (47-101)	64 (48-100)
F stages		
F0	0	
F1	32 (50.8%)	
F2	21 (33.3%)	
F3	9 (14.3%)	
F4		19
HCV RNA		
high	52 (82.5%)	17 (89.5%)
low	11 (17.5%)	2 (10.5%)
Serotype		
1	41 (49.4%)	12 (14.5%)
2	22 (26.6%)	7 (8.4%)

p was obtained using the Mann–Whitney U test,

Abbreviations: BCAA, branched chain amino acids; BTR, BCAA to tyrosine molar ratio; CH, chronic hepatitis; LC, liver cirrhosis; AST, aspartate amino transferase; ALT, alanine aminotransferase; ALP, alkaline phosphatase; Γ-GT, γ-glutamyltransferase; ICGR15, the retention rate of indocyanine green at 15 min, HCV RNA high, ≥10^6copy/mL; HCV RNA low, <10^5copy/mL

Clinical and laboratory evaluation of patients with CHC and LC

Serum and liver biopsy specimens were collected at the time of liver biopsy and stored at −80°C until analysis. Samples were only collected from the patients who provided informed consent for their serum samples to be stored for subsequent laboratory analysis. The exclusion criteria for CHC and LC were as follows: age < 18 years, habitual alcohol consumption (> 30 g ethanol/day), presence of hepatitis B surface antigen (enzyme-linked immunosorbent assay (ELISA); Abbott Tokyo, Japan), presence of anti-smooth muscle antibody (fluorescent antibody method; FA), presence of anti-mitochondrial M2 antibody (enzyme immunoassay; EIA), and current intravenous drug use. All patients were positive for serum HCV RNA and were followed up for > 1 year. A definitive diagnosis of HCC was obtained using abdominal angiography or liver tumor biopsy. HCC nodules were evaluated every 3–12 months if detected using contrast-enhanced abdominal ultrasonography or enhanced CT. All patients were closely followed up for HCC development at our outpatient clinic until May 31, 2020.

Hematological and biochemical examinations

The serum concentrations of aspartate aminotransferase (AST), alanine aminotransferase (ALT), alanine phosphatase (ALP), γ-glutamyl transpeptidase (γ-GT), total bilirubin, total protein (TP), albumin (Alb), branched-chain amino acid-to-tyrosine molar ratio (BTR), prothrombin time (PT), platelet count, and zinc were evaluated. In addition, the serum concentration of alpha-fetoprotein (AFP) was measured as a tumor marker, and the indocyanine green retention rate at 15 min (ICGR15) was also assessed. Serum zinc concentrations were determined using conventional atomic absorption spectrophotometry with a Zeeman polarized atomic absorption spectrophotometer (Z-6100; Hitachi, Tokyo, Japan). Serum ferritin levels were assessed using chemiluminescent ELISA or EIA (SRL, Tokyo, Japan). Serum levels of HCV RNA were determined using the Amplicor HCV Monitor (Roche Diagnostics KK, Tokyo, Japan) or TaqMan PCR methods (Cobas TaqMan HCV [auto] v2.0; Roche Diagnostics KK, Tokyo, Japan). Each patient's serum HCV RNA level was classified as high (≥100 kilo copies/mL or 5.0 log U/mL) or low (<100 kilo copies/mL or 5.0 log U/mL). The HCV serotype was determined using an EIA kit (Imucheck F-HCV Gr1 and Gr2 reagents; International Reagent Corporation, Tokyo, Japan) according to the manufacturer's instructions.

Histological analysis of hematoxylin-eosin-stained sections from liver biopsy

Liver biopsy specimens were obtained from patients with CHC or LC through percutaneous needle biopsy (Tru-Cut soft tissue biopsy needles, 14 G, Baxter, Deerfield, IL, USA) or hard Monopty needles (14 G, Medicon, Tokyo, Japan). These sections were fixed in 10%–20% buffered formalin and embedded in paraffin. The paraffin-embedded specimens were cut into 3- to 4-μm sections and stained with hematoxylin and eosin (HE). Each liver biopsy specimen was analyzed semi-quantitatively, with a score assigned to each parameter, as previously reported [25,27,30]. The HE-stained sections obtained from the liver biopsies performed at our department were evaluated by the first author and co-authors at a conference without knowledge of the patients' characteristics. The data were entered into a database and subsequently relevant patient data were retrieved from the database and analyzed.

Real-time quantitative PCR analysis

Hepcidin mRNA expression was evaluated using real-time reverse transcription-quantitative polymerase chain reaction (RT-qPCR). RNA was extracted from the liver using TRIzol reagent (Thermo Fisher Scientific, Waltham, MA, U.S.A.) [27]. Complementary DNA was synthesized from 4 μg of total RNA using the SuperScript ™ III First-Strand Synthesis System (Thermo Fisher Scientific). qPCR was performed using a THUNDERBIRD® SYBR qPCR Mix (TOYOBO, Osaka, Japan) and a 7500 Fast Real-Time PCR System (Thermo Fisher Scientific). Gene expression was normalized to GAPDH expression. The qPCR conditions included 95°C for 1 min, followed by 40 cycles of 95°C for 15 s, and 60°C for 60 s. The RT-qPCR data were analyzed using a standard curve. The correlation coefficient of the standard curve was > 0.90 for all patients. The PCR primer sequences used for detection were hepcidin F (5′-CAC AAC AGA CGG GAC AAC TT-3′; 20-mer), hepcidin R (5′-CGC AGC AGA AAA TGC AGA TG-3′; 20-mer), GAPDH F (5′- TGA Superscript CAT CAA GAA GGT Superscript GAA G -3′; 25-mer), and GAPDH R (5′- TCC TTG GAG GCC ATG TGG GCC AT -3′; 23-mer). The expression of *hepcidin* mRNA was quantified using the formula: $\Delta Ct = Ct_{\text{for hepcidin gene test}} - Ct_{GAPDH\,test}$. The RT-qPCR experiments were performed in triplicate.

Long-term patient outcomes

In order to assess long-term patient outcomes, we compared the cumulative probability of HCC based on the classification of *hepcidin* mRNA expression (ΔCt) as high or low. The high ΔCt group included patients with *hepcidin* ΔCt levels exceeding the middle value for all patients, while the low ΔCt group included those with *hepcidin* ΔCt levels below the middle level.

Measurement of serum cytokine and chemokine concentrations

Cytokine and chemokine levels in the serum of 49 patients were measured using a Bio-plex Suspension Array System (Bio-Rad Laboratories, HERCULES, CA, USA) following concentrations measured in our previous study [30]. The cytokines and chemokines measured were cutaneous T-cell-attracting chemokine (CTACK), growth-regulated alpha protein (GROa), interleukin (IL)-1α, IL-2 receptor α(Rα), IL-3, IL-12p40, IL-16, IL-18, leukemia inhibitory factor (LIF), monocyte-specific chemokine 3 (MCP-3), macrophage colony-stimulating factor (M-CSF), macrophage migration inhibitory factor (MIF), Hu migration inducing gene (MIG), b-nerve growth factor (NGF), c-Kit receptor present on mast cells and stem cell factor (SCF), stem cell growth factor β(SCGF)-β, stromal cell-derived factor 1 α (SDF-1α), tumor necrosis factor (TNF)-β, tumor necrosis factor-related apoptosis-inducing ligand (TRAIL), hepatocyte growth factor (HGF), Hu interferon α2 (IFN-α2), platelet-derived growth factor receptor (PDGF)- ββ, IL-1b, IL-1ra, IL-2, IL-4, IL-5, IL-6, IL-7, IL-8, IL-9, IL-10, IL-12(p70), IL-13, IL-15, IL-17, eotaxin, FGF basic, granulocyte-colony stimulating factor (G-CSF), granulocyte macrophage-colony stimulating factor (GM-CSF), interferon gamma (IFN-γ), interferon gamma-induced protein-10 (IP-10), monocyte chemoattractant protein-1 (MCP-1)(MCAF), macrophage inflammatory protein 1 (MIP-1α), MIP-1β, regulated on activation normal T-cell expressed and secreted (RANTES), TNF-α, and vascular endothelial growth factor (VEGF).

Statistical analysis

Statistical analysis was performed using JMP 12 software (SAS Institute Inc., Tokyo, Japan). Data are expressed as the mean ± SD or median (range). Categorical variables were compared using the Mann–Whitney U test (non-parametric). The Kruskal–Wallis and Steel–Dwass tests were used for multiple-group comparisons. The Spearman's rank correlation coefficient test was used for correlation analysis between the two groups. $p < 0.05$ was considered statistically significant. The cumulative incidence of HCC development was estimated using the Kaplan–Meier method, and differences between groups were assessed using the log-rank test. Statistical analyses was performed using JMP 12 software (SAS Institute Inc., Tokyo, Japan).

Ethical Approval

This study was approved by the Ethics Committee of Nihon University School of Medicine (RK-100611-13, # RK100910-15) and conducted in accordance with the tenets of the Declaration of Helsinki of 1964 and its subsequent amendments. Written informed consent was obtained from all participants. The enrolled patients agreed to cooperate with the study procedures and for publication of the results.

Results

Hepcidin mRNA expression (ΔCt) levels of liver biopsy specimens obtained from patients with CHC or LC

The median levels of *hepcidin* (ΔCt) did not show any significant differences between the sexes or between different age groups. Additionally, no significant differences were observed in the median *hepcidin* ΔCt levels between patients with different stages of chronic liver disease (F0 to F4) or between different HCV serotypes or serum HCV RNA levels (**Table 2**).

Correlation between *hepcidin* ΔCt levels and blood, biochemical, and histological parameters

Hepcidin ΔCt levels did not exhibit significant correlations with most biochemical parameters, except for serum ferritin concentration (r=−0.357; p=0.0161) and unsaturated iron binding capacity (p=0.0003; **Table 3**). Interestingly, *hepcidin* ΔCt levels did not show any significant associations with the scores of histological factors, although a significant correlation was observed between the extent of POAH and *hepcidin* ΔCt levels (r=0.288, p=0.0086). Patients with higher *hepcidin* ΔCt levels were more likely to exhibit a greater degree of POAH (minimal versus moderate, p=0.0158; none versus moderate, p=0.0242, **Figure 1A**). Notably, no significant association was observed between *hepcidin* ΔCt levels and the F-stages (p=0.3254; **Figure 1B**).

Table 2. | Associations between *hepcidin* mRNA expression (ΔCt) and clinical characteristics of patients (n=82).

Parameter	number	r	*p*
Gender			0.5223
male	44	0.0744	
female	38	0.4817	
Age			0.0669
<65 yrs	66	0.2139	
≥65 yrs	16	1.3036	
Genotype			0.9200
1a	54	0.3267	
2a	15	0.5013	
2b	12	−0.1300	
HCV RNA			0.3351
High	67	0.5012	
Low	12	−0.2411	

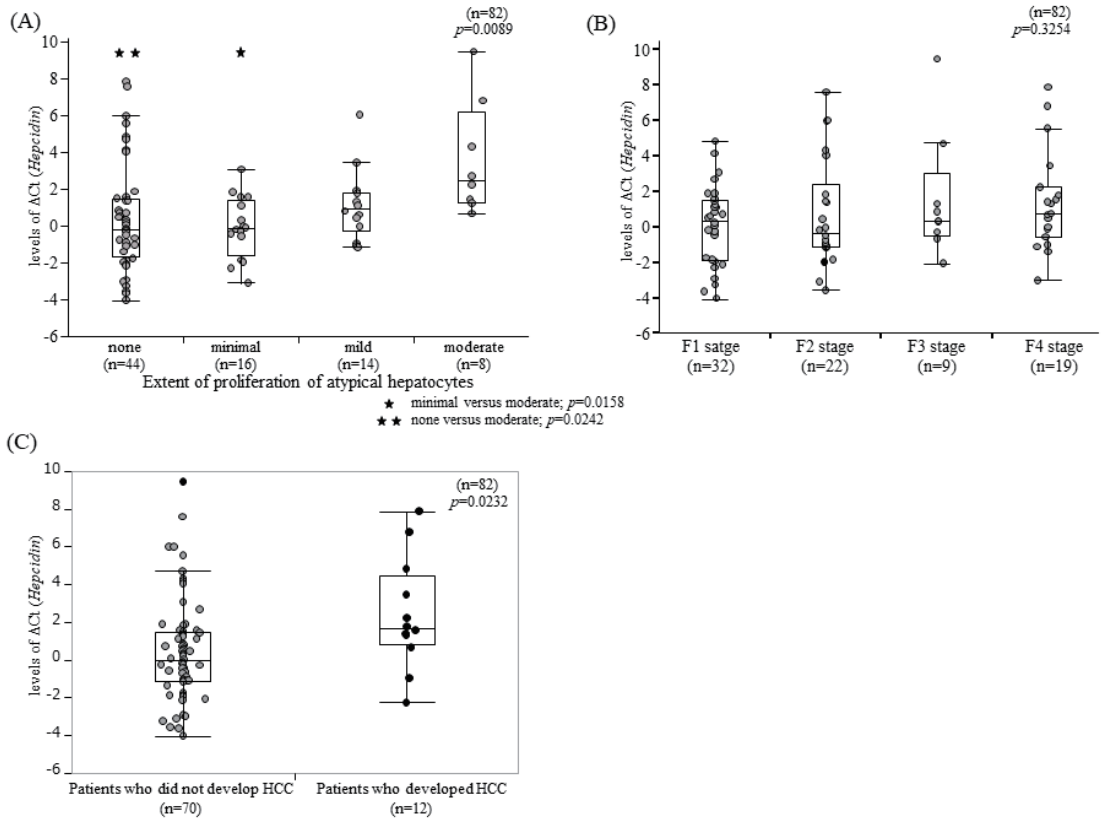

Figure 1. (A) *Hepcidin* mRNA expression was quantified using the formula: $\Delta Ct = Ct_{\text{for hepcidin gene test}} - Ct_{\text{glyceraldehyde-3-phosphate dehydrogenase (GAPDH) test}}$. The degree of proliferation of atypical hepatocytes (POAH) and *hepcidin* ΔCt levels were significantly associated with the degree or extent of POAH (p=0.0089) based on robust regression analysis using Huber M estimation. Significant differences in *hepcidin* ΔCt levels were observed between moderate and minimal (p=0.0158) and none and moderate (p=0.0242) POAH, with *hepcidin* ΔCt levels being significantly higher in moderate cases (p=0.0267) based on Kruskal–Wallis and Steel–Dwass tests.

(B) Comparison between *hepcidin* ΔCt levels and F1 to F4 stages in patients with hepatitis C virus (HCV) RNA-positive chronic hepatitis. No significant correlation was observed between *hepcidin* ΔCt level and F stage (p=0.3254). Data were analyzed using Kruskal–Wallis and Steel–Dwass tests.

(C) Comparison between *hepcidin* ΔCt levels and the development of hepatocellular carcinoma in patients. Patients who did not develop HCC exhibited significantly lower *hepcidin* ΔCt levels than those who developed HCC (p=0.0232). Data were analyzed using ANOVA.

Table 3. Associations between *hepcidin* mRNA expression levels (ΔCt), blood and biochemical examination results or histological parameters of patients (n=82)

Parameter	number	r	*p*
Blood and Serological Examination.			
aspartate aminotransferase (U/L)	82	0.100	0.367
alanine aminotransferase (U/L)	82	0.017	0.875
γ-glutamyl transpeptidase (U/L)	82	−0.114	0.306
alkaline phosphatase (U/L)	82	−0.099	0.306
total Bilirubin (mg/dl)	82	−0.176	0.112
platelet counts (x10^4)	82	−0.020	0.852
total protein (g/dl)	74	0.023	0.837
albumin (g/dl)	74	−0.151	0.210
prothrombin time (%)	74	0.031	0.779
BTR	62	−0.135	0.315
BCAA	62	0.089	0.508
tyrosine	62	0.191	0.153
indocyanine green retention rate 15min	62	0.043	0.700
alpha-feto protein (ng/ml)	70	0.029	0.798
zinc concentration (μg/ml)	62	−0.013	0.914
ferritin concentration (ng/ml)	62	−0.382	0.009
FIB-4	82	0.178	0.123
APRI	82	0.141	0.221
unsaturated iron binding capacity	62	0.582	0.0003
Histology of liver biopsy section (score)	82		
Irregular regeneration of hepatocytes	82		
anisocytosis of hepatocytes		0.084	0.448
bulging of hepatocytes		0.106	0.341
map-like distribution		0.123	0.269
oncocytic change of hepatocytes		0.089	0.424
nodular arrangement of hepatocytes		0.136	0.052
proliferation of atypical hepatocytes		0.288	0.0086
Inflammatory cell infiltration			
peri-portal		0.101	0.366
parenchyma		0.138	0.215
portal		−0.044	0.692
F stage		0.144	0.196
lymphoid aggregation of portal tract		−0.020	0.858
portal sclerotic change		−0.068	0.563
bile duct damage		−0.124	0.266
peri-venular fibrosis		−0.150	0.177
peri-cellular fibrosis		0.005	0.958
bridging necrosis		0.002	0.858
steatosis		0.173	0.118

Data were analyzed using Spearman's rank correlation coefficients. Abbreviations: BCAA, branched-chain amino acids; BTR, BCAA-to-tyrosine molar ratio, FIB-4; fibrosis-4; APRI, AST-to-platelet ratio index.

Correlations between *hepcidin* ΔCt levels and HCC development in patients

The relationship between *hepcidin* ΔCt levels and the development of HCC was analyzed in patients, and revealed that the levels of *hepcidin* ΔCt in the liver biopsy specimens of patients who developed HCC were significantly higher than those of patients who did not develop HCC (p=0.0232; **Figure 1C**).

Relationship between *hepcidin* ΔCt levels and cumulative incidence of HCC development

The cumulative incidence of HCC development was analyzed in the cohort of 82 patients. These patients were divided into low (<0.299) and high (≥0.334) groups based on their *hepcidin* ΔCt levels. The low ΔCt group consisted of patients with *hepcidin* ΔCt expression below the middle value, whereas the high ΔCt group comprised patients with *hepcidin* ΔCt expression exceeding the middle level. The cumulative incidence of HCC in the low ΔCt group, after a median follow-up of 12.06 (range: 0.11–18.71) years, was significantly lower than that in the high ΔCt group, with a median follow-up of 8.13 (range: 0.32–17.18) years (p=0.0028; **Figure 2A**). Moreover, the 5-year incidence rates were 0% and 19.2% in the low and high ΔCt groups, respectively. The association between *hepcidin* ΔCt levels in patients who developed HCC and the time to HCC development after the first liver biopsy was then examined. Although no statistically significant difference was observed, there was a tendency for a shorter time to HCC development in patients with low *hepcidin* ΔCt levels (p=0.3675; **Figure 2B**). These findings suggest that higher *hepcidin* ΔCt levels are associated with an increased risk of HCC development.

Correlations between serum cytokine/chemokine concentrations and *hepcidin* ΔCt levels

Significant correlations were observed between *hepcidin* ΔCt levels and the concentrations of certain cytokines (**Table 4**). The *hepcidin* ΔCt levels was positively correlated with the concentrations of IL-1α (r=0.3323; p=0.0197), IL-5 (r=0.3771; p=0.0076), IL-8 (r=0.2823; p =0.0493), IL-10 (r=0.3395; p=0.0170), IL-12 (p70) (r=0.4243; p=0.0024), IL-13 (r=0.3110; p =0.0024), G-CSF (r=0.3294; p=0.0208), GM-CSF (r=0.3208; p=0.0246), IFN-γ (r=0.3063; p=0.0323), MIP-1b (r=0.2840; p=0.0480). Conversely, a negative correlation was observed between *hepcidin* ΔCt levels and the concentration of TRAIL (r=−0.2933, p=0.0408).

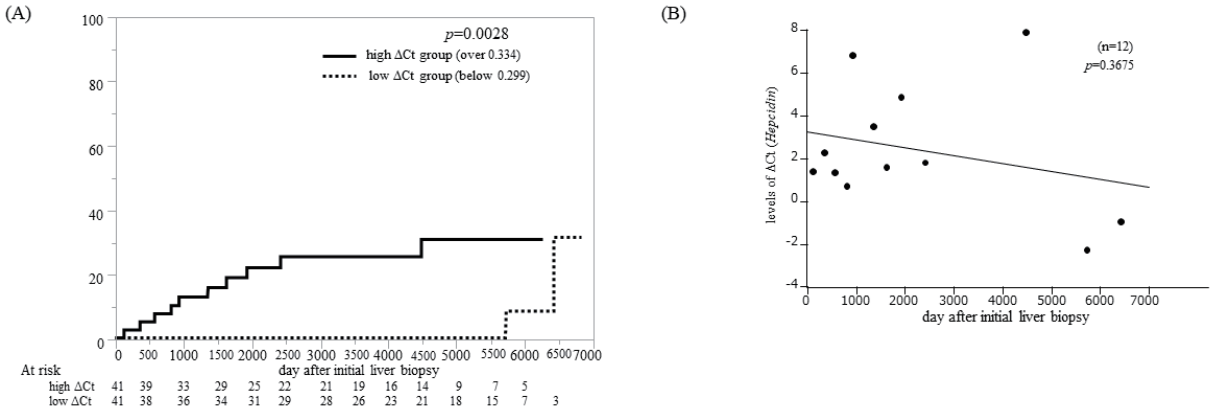

Figure 2. (A) The cumulative incidence of HCC development in the high *hepcidin* ΔCt group (≥0.334, straight line) was significantly higher than that in the low *hepcidin* ΔCt group <0.299, dashed line) (p=0.0028). Data were analyzed using the Kaplan–Meier method, and between-group differences were assessed using the log-rank test.
(B) Comparison between days after initial biopsy during HCC development and *hepcidin* ΔCt levels (p=0.3675). Data were analyzed using Spearman's rank correlation test.

Table 4. Associations between *hepcidin* levels (ΔCt) and serum cytokine and chemokine concentrations (n=49). The expression of each gene mRNA was quantified using the formula: $\Delta Ct = Ct_{\text{for each gene test}} : Ct_{\beta\text{-actin}}$. RT-qPCR experiments were performed in triplicate.

	r	*p*		r	*p*
Hu CTACK	−0.0407	0.7812	Hu IL-2	0.2238	0.1222
Hu GROa	0.1041	0.4766	Hu IL-4	0.0254	0.8624
Hu IL-1α	0.3323	0.0197	Hu IL-5	0.3771	0.0076
Hu IL-2Ra	0.2457	0.0888	Hu IL-6	0.2791	0.0521
Hu IL-3	0.1984	0.1717	Hu IL-7	0.2149	0.1381
Hu IL-12p40	0.0416	0.7766	Hu IL-8	0.2823	0.0493
Hu IL-16	0.0280	0.8485	Hu IL-9	0.0889	0.5436
Hu IL-18	0.0272	0.8526	Hu IL-10	0.3395	0.0170
Hu LIF	−0.0367	0.8024	Hu IL-12(p70)	0.4243	0.0024
Hu MCP-3	0.0958	0.5126	Hu IL-13	0.3110	0.0296
Hu M-CSF	0.1273	0.3834	Hu IL-15	0.1814	0.2122
Hu MIF	0.0861	0.5565	Hu IL-17	0.1021	0.4851
Hu MIG	0.2319	0.1088	Hu Eotaxin	0.0131	0.9290
Hu b-NGF	0.1598	0.2726	Hu FGF basic	−0.1754	0.2280
Hu SCF	−0.0669	0.6477	Hu G-CSF	0.3294	0.0208
Hu SCGF-b	0.0456	0.7556	Hu GM-CSF	0.3208	0.0246
Hu SDF-1a	0.1161	0.4270	Hu IFN-γ	0.3063	0.0323
Hu TNF-β	0.2257	0.8692	Hu IP-10	0.0033	0.9820
Hu TRAIL	−0.2933	0.0408	Hu MCP-1(MCAF)	0.1930	0.1841
Hu HGF	0.0583	0.6909	Hu MIP-1a	−0.1451	0.3200
Hu IFN-a2	0.1822	0.2103	Hu MIP-1b	0.2840	0.0480
Hu PDGF-bb	0.0384	0.7935	Hu RANTES	0.1317	0.3669
Hu IL-1b	0.2537	0.0797	Hu TNF-alpha	0.2411	0.0952
Hu IL-1ra	−0.0337	0.8183	Hu VEGF	0.1174	0.4216

The expression of each gene mRNA was quantified using the formula: $\Delta Ct = Ct_{\text{for each gene test}} : Ct_{\beta\text{-actin}}$. RT-qPCR experiments were performed in triplicate. The following cytokines and chemokines were measured: cutaneous T-cell-attracting chemokine (CTACK), growth-regulated alpha protein (GROa), Interleukin (IL)-1α, IL-2 receptor α(Rα), IL-3, IL-12p40, IL-16, IL-18, leukemia Inhibitory Factor (LIF), monocyte-specific chemokine 3 (MCP-3), macrophage colonystimulating factor (M-CSF), macrophage migration inhibitory factor (MIF), Hu migration inducing gene (MIG), b-nerve growth factor (NGF), c-Kit receptor present on mast cells and stem cell factor (SCF), stem cell growth factor β(SCGF)-β, stromal cell-derived factor 1 α (SDF-1α), tumor necrosis factor (TNF)-β, tumor necrosis factor-related apoptosis-inducing ligand (TRAIL), hepatocyte growth factor (HGF), Hu interferon α2 (IFN-α2), platelet-derived growth factor receptor (PDGF)- ββ, IL-1b, IL-1ra, IL-2 , IL-4, IL-5, IL-6, IL-7, IL-8 , IL-9, IL-10, IL-12(p70), IL-13, IL-15, IL-17, eotaxin, FGF basic, granulocyte-colony stimulating factor (G-CSF), granulocyte macrophage-colony stimulating factor (GM-CSF), interferon gamma (IFN-γ), interferon gamma-induced protein-10 (IP-10), monocyte chemoattractant protein-1 (MCP-1)(MCAF), macrophage inflammatory protein 1 (MIP-1α), MIP-1β, regulated on activation, normal T-cell expressed and secreted (RANTES), TNF-α, and vascular endothelial growth factor (VEGF).

Discussion

The results of our study suggest that patients with low *hepcidin* mRNA expression in liver biopsy tissues are at higher risk of developing HCC. This is supported that the majority of patients who developed HCC exhibited high *hepcidin* ΔCt levels. Previous studies have reported a reduction in *hepcidin* mRNA expression in HCC tissues compared to that in non-cancerous liver tissues [31,32].

Based on the premise that low *hepcidin* mRNA expression (high *hepcidin* ΔCt level) is a risk factor for HCC development, we propose a hypothesis regarding the underlying mechanism. We hypothesize that within the lobules of patients with chronic hepatitis or cirrhosis, some of the atypical regenerating hepatocytes are more similar to HCC cells than to normal hepatocytes. Consequently, these hepatocytes may possess a diminished capacity to produce *hepcidin* mRNA. This may explain the observed decrease in *hepcidin* mRNA expression under these conditions. Based on our hypothesis, we speculate that livers with low *hepcidin* mRNA expression may have atypical hepatocytes that exhibit similar characteristics to those of HCC cells to some extent, when compared to normal hepatocytes.

Although the frequency of patients with advanced POAH was low, those with mild or higher POAH exhibited significantly lower *hepcidin* mRNA expression (**Figure 1A**). To date, we have reported the extent of POAH as a risk factor for the development of HCC from chronic hepatitis C and as a risk factor for HCC recurrence [33,34]. This suggests that hepcidin may play a direct role in the development of POAH. Further investigation is required for more detailed exploration of this hypothesis, which is beyond the scope of the present study. Our results support the finding that low hepcidin expression in cancerous areas is associated with HCC progression and poor prognosis [34,35].

While low *hepcidin* mRNA expression in liver tissue is a significant predictor of HCC development, the exact role of hepcidin in inhibiting or promoting HCC development remains unclear. Further studies are required to elucidate the precise mechanisms and determine the specific impact of hepcidin on HCC development. Furthermore, *hepcidin* mRNA expression showed an inverse positive correlation with blood ferritin concentration and a positive correlation with unsaturated iron-binding capacity levels, although only a few patients were analyzed. Based on this finding, it appears plausible that blood ferritin concentration reflects *hepcidin* mRNA expression in liver biopsy tissues. However, it is important to note that blood ferritin levels may be elevated under carcinogenic conditions or in patients with high levels of inflammation. Therefore, caution should be exercised when interpreting the blood ferritin level as a direct indicator of *hepcidin* mRNA expression in the liver. In contrast, *hepcidin* mRNA expression was not associated with the degree of inflammatory lymphocytic infiltration in liver lobules. This finding may suggests that *hepcidin* mRNA expression is unrelated to the mechanism of hepatocellular injury recognized by immunocompetent cells. In general, low *hepcidin* mRNA expression in hepatocytes indicates that ferroportin expression is not suppressed, thereby resulting in an increased export of iron ions from the cells, leading to a reduction in the intracellular iron ion levels. Hence, the reduction of iron ions can be seen as a mechanism that aids in suppressing the generation of radicals that can cause cellular damage.

We further investigated the relationship between serum cytokine and chemokine concentrations and *hepcidin* mRNA expression levels in the liver biopsy tissues. We found that *hepcidin* mRNA expression positively correlated with TRAIL only. On the other hand, *hepcidin* mRNA expression exhibited inverse correlations with IL-1α, IL-5, IL-8, IL-10, IL-12 (P40), IL-13, G-CSF, GM-CSF, IFN-γ, and MIP-1b. These findings suggest a complex interplay between *hepcidin* mRNA expression and various cytokines and chemokines in the liver microenvironment. The lifespan of neutrophils is normally 2–3 days at most to induce apoptosis, and the inverse correlation between G-CSF and GM-CSF suggests that low *hepcidin* mRNA expression may induce apoptosis and respond to infection by increasing the production of the granulocyte lineage and monocytes. Further, TRAIL is an antitumor cytokine that transduces apoptosis-inducing signals into cells by binding to specific receptors on the cell membrane [35]. Therefore, the positive correlation between *hepcidin* mRNA expression and TRAIL may indicate a pro-apoptotic effect of hepcidin. Zerafa et al. reported that TRAIL-knockout mice exhibit increased rates of carcinogenesis [36], and this positive correlation also suggests that hepcidin may exert an inhibitory effect on hepatocarcinogenesis. Thus, *hepcidin* mRNA levels positively correlated with TRAIL and negatively correlated with IL-13 and G-CSF, suggesting that hepcidin regulates apoptosis in a hyperactivating direction. Next, *hepcidin* mRNA expression was inversely correlated with MIP-1β (CCL4). Although MIP-1α/β display similar responses, MIP-1 selectively induces migration of CD8+ lymphocytes and MIP-1β of CD4+ lymphocytes [37]. Additionally, MIP-1 (CCL4) promotes tumor development and progression by recruiting regulatory T cells and pro-tumorigenic macrophages to enhance their pro-tumorigenic capacity [38]. IL-10 acts on immune cells such as

T cells and macrophages, directly suppressing cell activation and weakening the antigen-presenting capacity of macrophages, thereby suppressing the immune response [39]. IL-12 (p70) is a cytokine essential for the induction of Th1 responses through the production of IFN-γ, which is important for protective immunity against infection and the induction of tumor immunity [40]. IL-13 has been observed to be a mediator of cytotoxicity *in vitro* and it has been reported that IL-13 induces cell death when applied to the colon cancer epithelial cell line HT29 [41,42]. It is believed that the disruption of the cell structure by IL-13 causes unstable cells to undergo apoptosis. Taken together, these results suggest that low *hepcidin* mRNA expression facilitates the enhancement of cell apoptosis and may also modulate the inflammatory response in an inhibitory manner. Comparison of cytokine/chemokine concentrations requires the detection of *hepcidin* mRNA expression and cytokine/chemokine levels in the liver tissue. To further elucidate the function of hepcidin and the mechanisms regulating *hepcidin* mRNA expression, we compared the differences in hepcidin expression in cell lines in which hepcidin was highly expressed in cultured cells or knocked down using small interfering RNA, and performed RNA-Seq to confirm the differences in gene expression. This study was based on a small number of liver biopsy tissues. We would like to recruit more patients and perform further studies using more liver tissue samples.

In conclusion, this study suggests that low *hepcidin* mRNA expression in patients with HCV-associated liver disease is associated with a high risk of HCC development. Thus, low *hepcidin* mRNA expression appears to indicate a hypercarcinogenic liver state. Furthermore, measuring *hepcidin* mRNA expression can be clinically useful for predicting the long-term prognosis of patients and for guiding treatment decisions.

Acknowledgments

We greatly thanks for Motomi Yamazaki, PhD. And Ms. Kayo Iwaguchi, and Ms. Shinobu Arai for technical assistance.

Author Contributions:

M.O. and M.M., contributed to data collection, statistical analyses, interpretation of data, the writing of the manuscript and was the main author of the manuscript.
M.O., H.N, and M.M., contributed to data and sample collection,
M.O., M.M., and K.K. were contributed for study concept and design;
H.N. and M.M. were contributed for histological analysis;
M.M., T.S. and K.K. were responsible or analysis and interpretation of data;
M.M., and K.K. were responsible for statistical analysis;

Ethics approval and consent to participate:

This study was approved by the Ethics Committee of Nihon University School of Medicine (RK-100611-13, # RK100910-15). The study was performed in accordance with the ethical standards as laid down in the 1964 Declaration of Helsinki and its later amendments or comparable ethical standards.

Consent for participate: Written informed consent was obtained from each patient.

Availability of data and material: Not applicable.

Funding: Not applicable.

Consent for publication: Not applicable.

References

[1] Billesbølle CB, Azumaya CM, Kretsch RC, Powers AS, Gonen S, Schneider S, Arvedson T, Dror RO, Cheng Y, Manglik A. Structure of hepcidin-bound ferroportin reveals iron homeostatic mechanisms. *Nature*. 2020; 586(7831):807-811. doi: 10.1038/s41586-020-2668-z. Epub 2020 Aug 19.

[2] Nemeth E et al. Hepcidin regulates cellular iron efflux by binding to ferroportin and inducing its internalization. Science. 2004; 306, 2090-2093.

[3] Aschemeyer S et al. Structure-function analysis of ferroportin defines the binding site and an alternative mechanism of action of hepcidin. Blood, *The Journal of the American Society of Hematology*. 2018; 131, 899-910.

[4] De Domenico I et al. The molecular mechanism of hepcidin-mediated ferroportin down-regulation. Mol. Biol. Cell. 2007; 18, 2569-2578.

[5] Qiao B et al. Hepcidin-induced endocytosis of ferroportin is dependent on ferroportin ubiquitination. Cell Metab. 2012; 15, 918-924.

[6] Ross SL et al. Molecular mechanism of hepcidin-mediated ferroportin internalization requires ferroportin lysines, not tyrosines or JAK-STAT. *Cell Metab*. 2012; 15, 905-917.

[7] Darshan D, Anderson GJ. Interacting signals in the control of hepcidin expression. *Biometals*. 2009; 22: 77-87.

[8] Mastrogiannaki M, Matak P, Keith B, Simon MC, Vaulont S, Peyssonnaux C. HIF-2alpha, but not HIF-1alpha, promotes iron absorption in mice. *J Clin Invest*. 2009; 119: 1159-1166.

[9] Sagar P, Angmo S, Sandhir R, Rishi V, Yadav H, Singhal NK. Effect of hepcidin antagonists on anemia during inflammatory disorders. *Pharmacol Ther*. 2021; 226: 107877.

[10] Miyachi H, Kobayashi Y, Relja B, Fujita N, Iwasa M, Gabazza EC, Takei Y. Effect of suppressor of cytokine signaling on hepcidin production in hepatitis C virus replicon cells. *Hepatol Res*. 2011 ; 41: 364-374.

[11] Mifuji-Moroka R, Iwasa M, Miyachi H, Sugimoto R, Tanaka H, Ishihara T, Fujita N, Kaito M, Kobayashi Y, Takei Y. Iron overload and glucose abnormalities in chronic hepatitis C virus infection: phlebotomy lowers risk of new-onset diabetes. *Hepatogastroenterology*. 2013; 60: 1736-1741.

[12] Kohgo Y, Ikuta K, Ohtake T, Torimoto Y, Kato J. Iron overload and cofactors with special reference to alcohol, hepatitis C virus infection and steatosis/insulin resistance. *World J Gastroenterol*. 2007;13 : 4699-706.

[13] Higuchi T, Moriyama M, Fukushima A, Matsumura H, Matsuoka S, Kanda T, Sugitani M, Tsunemi A, Ueno T, Fukuda N. Association of mRNA expression of iron metabolism-associated genes and progression of non-alcoholic steatohepatitis in rats. *Oncotarget*. 2018; 9: 26183-26194.

[14] Chen H, Zhao W, Yan X, Huang T, Yang A. Overexpression of Hepcidin Alleviates Steatohepatitis and Fibrosis in a Diet-induced Nonalcoholic Steatohepatitis. *J Clin Transl Hepatol.* 2022; 10: 577-588.

[15] Datz C, Müller E, Aigner E. Iron overload and non-alcoholic fatty liver disease. *Minerva Endocrinol.* 2017; 42: 173-183.

[16] Corradini E, Pietrangelo A. Iron and steatohepatitis. *J Gastroenterol Hepatol.* 2012; 27 Suppl 2:42-46.

[17] Abd Elmonem E, Tharwa el-S, Farag MA, Fawzy A, El Shinnawy SF, Suliman S. Hepcidin mRNA level as a parameter of disease progression in chronic hepatitis C and hepatocellular carcinoma. *J Egypt Natl Canc Inst*. 2009; 21: 333-42.

[18] Aoki CA, Rossaro L, Ramsamooj R, Brandhagen D, Burritt MF, Bowlus CL. Liver hepcidin mRNA correlates with iron stores, but not inflammation, in patients with chronic hepatitis C. *J Clin Gastroenterol*. 2005; 39: 71-74.

[19] Nirei K, Matsuoka S, Nakamura H, Matsumura H, Moriyama M. Incidence of hepatocellular carcinoma reduced by phlebotomy treatment in patients with chronic hepatitis C. *Intern Med*. 2015; 54: 107-117.

[20] Chino S, Moriyama M, Matsumura H, Ono Y, Arakawa Y. Clinical pathological significance of iron metabolism with chronic hepatitis C patients. *Hepatol Res*. 2002; 24: 245.

[21] Uchida T. Small hepatocellular carcinoma: its relationship to multistep hepato-carcinogenesis. *Pathol Int*. 1995; 45:175-184.

[22] Uchida T. Pathology of hepatitis C. *Intervirology*. 1994; 37: 126-132.

[23] Shibata M, Morizane T, Uchida T, Yamagami T, Onozuka Y, Nakano M, et al. Irregular regeneration of hepatocytes and risk of hepatocellular carcinoma in chronic hepatitis and cirrhosis with hepatitis-C-virus infection. *Lancet.* 1998; 351: 1773-1777.

[24] Peters RL. Viral hepatitis: a pathologic spectrum. *Am J Med Sci.* 1975; 270:17-31.

[25] Matsumura H, Nirei K, Nakamura H, Higuchi T, Arakawa Y, Ogawa M, Tanaka N, Moriyama M. Histopathology of type C liver disease for determining hepatocellular carcinoma risk factors. *World J Gastroenterol*. 2013; 19: 4887-4896.

[26] Ueno Y, Moriyama M, Uchida T, Arakawa Y. Irregular regeneration of hepatocytes is an important factor in the hepatocarcinogenesis of liver disease. *Hepatology.* 2001; 33: 357-362.

[27] Moriyama M, Kanda T, Midorikawa Y, Matsumura H, Masuzaki R, Nakamura H, Ogawa M, Matsuoka S, Shibata T, Yamazaki M, Kuroda K, Nakayama H, Higaki T, Kanemaru K, Miki T, Sugitani M, Takayama T. The proliferation of atypical hepatocytes and CDT1 expression in noncancerous tissue are associated with the postoperative recurrence of hepatocellular carcinoma. *Sci Rep*. 2022; 12: 20508. doi: 10.1038/s41598-022-25201-6

[28] Ichida F, Tsuji T, Omata M, Ichida T, Inoue K, Kamimura T, Yet al. New Inuyama classification: new criteria for histological assessment of chronic hepatitis. *Int Hepatol Commun* 1996; 6: 112-119.

[29] Desmet VJ, Gerber M, Hoofnagle JH, Manns M, Scheuer PJ. Classification of chronic hepatitis: diagnosis, grading and staging. *HEPATOLOGY* 1994; 19: 1513-1520.

[30] Ohnishi M, Higuchi A, Matsumura H, Arakawa Y, Nakamura H, Nirei K, Yamamoto T, Yamagami H, Ogawa M, Gotoda T, Matsuoka S, Nakajima N, Sugitani M, Moriyama M, Murayama H. Involvement of Ornithine Carbamoyltransferase in the Progression of Chronic Hepatitis C and Liver Cirrhosis. *Int J Med Sci*. 2017; 14: 629-638.

[31] Kijima H, Sawada T, Tomosugi N, Kubota K. Expression of hepcidin mRNA is uniformly suppressed in hepatocellular carcinoma. *BMC Cancer*. 2008 ; 8: 167.

[32] Kessler SM, Barghash A, Laggai S, Helms V, Kiemer AK. Hepatic hepcidin expression is decreased in cirrhosis and HCC. *J Hepatol*. 2015; 62: 977-979.

[33] Polak KZ, Schaffer P, Donaghy D, Zenk MC, Olver CS. Iron, hepcidin, and microcytosis in canine hepatocellular carcinoma. *Vet Clin Pathol*. 2022; 51: 208-215.

[34] Kessler SM, Barghash A, Laggai S, Helms V, Kiemer AK. Hepatic hepcidin expression is decreased in cirrhosis and HCC. *J Hepatol*. 2015; 62:977-979.

[35] Chaudhari BR, Murphy RF, Agrawal DK. Following the TRAIL to apoptosis. *Immunol Res*. 2006; 35: 249-262.

[36] Zerafa N, Westwood JA, Cretney E, Mitchell S, Waring P, Iezzi M, Smyth MJ. Cutting edge: TRAIL deficiency accelerates hematological malignancies. *J Immunol*. 2005; 175: 5586-5590.

[37] Obregon-Perko V, Hodara VL, Parodi LM, Giavedoni LD. Baboon CD8 T cells suppress SIVmac infection in CD4 T cells through contact-dependent production of MIP-1α, MIP-1β, and RANTES. *Cytokine*. 2018; 111: 408-419.

[38] Mukaida N, Sasaki SI, Baba T. CCL4 Signaling in the Tumor Microenvironment. *Adv Exp Med Biol*. 2020; 1231: 23-32.

[39] Minton K. Immune regulation: IL-10 targets macrophage metabolism. *Nat Rev Immunol.* 2017; 17: 345.

[40] Trinchieri G. Interleukin-12 and the regulation of innate resistance and adaptive immunity. *Nat Rev Immunol*. 2003; 3: 133-146.

[41] Li BH, Xu SB, Li F, Zou XG, Saimaiti A, Simayi D, Wang YH, Zhang Y, Yuan J, Zhang WJ. Stat6 activity-related Th2 cytokine profile and tumor growth advantage of human colorectal cancer cells in vitro and in vivo. *Cell Signal*. 2012; 24: 718-725.

[42] Wright K, Kolios G, Westwick J, Ward SG. Cytokine-induced apoptosis in epithelial HT-29 cells is independent of nitric oxide formation. Evidence for an interleukin-13-driven phosphatidylinositol 3-kinase-dependent survival mechanism. *J Biol Chem.* 1999; 274: 17193-201.

Regular Article https://metallomicsresearch.brte.org

Effects of genetic disruption in thioredoxin and glutathione systems on selenium nanoparticle formation, selenite sensitivity, and selenoprotein biosynthesis in *Escherichia coli*

Anna Ochi, Hisaaki Mihara*

Department of Biotechnology, College of Life Sciences, Ritsumeikan University, 1-1-1 Nojihigashi, Kusatsu, Shiga 525-8577, Japan

Abstract

Escherichia coli uses selenite as a nutritional selenium source for the synthesis of selenoproteins, and excess selenite is converted to elemental selenium nanoparticles (SeNPs) through a detoxification process. The reduction of selenite is thought to be facilitated by two major redox systems: the thioredoxin (Trx) system and glutathione (GSH) system. However, the extent to which these redox systems are involved in selenoprotein synthesis and SeNP formation remains unclear. In this study, we investigated the effects of gene disruption in the Trx (*trxA*, *trxB*, and *trxC*) and GSH (*gshB* and *gor*) systems on SeNP formation, selenite sensitivity, and selenoprotein synthesis in *E. coli*. We found that the disruption of a single gene in either the Trx or GSH system did not drastically affect SeNP formation via selenite reduction in the presence of 1 mM selenite. However, *trxB*, *gshB*, and *gor* were observed to be important for the tolerance of the bacterium to > 5 mM selenite. The Δ*trxA* and Δ*trxB* strains exhibited lower activity of the selenoprotein formate dehydrogenase as compared to the wild-type strain, suggesting that *trxA* and *trxB* are important for selenoprotein biosynthesis. Selenite detoxification via SeNP formation involves both the Trx and GSH systems, but selenoprotein biosynthesis specifically depends on the Trx system.

Keywords: selenite reduction, selenium nanoparticles, selenoprotein biosynthesis, *Escherichia coli*, thioredoxin, glutathione

Statements about COI: The authors have no conflicts of interest associated with this manuscript to declare.

Introduction

Selenium is an essential trace element found in many organisms [1-3]. It is primarily incorporated into selenoproteins as the 21st amino acid, selenocysteine (Sec) [4]. Selenoproteins include well-known examples such as formate dehydrogenase (FDH) and glycine reductase in bacteria as well as mammalian selenoprotein P and thioredoxin reductase [5, 6]. Although selenium plays a crucial role in biological processes, excess selenium can be toxic [1, 2, 7]. Several bacteria can reduce toxic selenium oxyanions, such as selenate (+VI) and selenite (+IV) [8]. This reduction is a part of their respiratory and detoxification mechanisms [9-11], leading to the formation of less toxic, insoluble elemental

*Correspondence:
Hisaaki Mihara
Department of Biotechnology, College of Life Sciences,
Ritsumeikan University, 1-1-1 Nojihigashi, Kusatsu,
Shiga 525-8577, Japan
Tel ; +81 77 561 2732
e-mail ; mihara@fc.ritsumei.ac.jp

Received: January 24, 2024
Accepted: March 19, 2024
Released online: April 3, 2024

 DOI https://doi.org/10.11299/metallomicsresearch.MR202401

selenium nanoparticles (SeNPs) [9] or their conversion into volatile methylated selenium species [12, 13].

The biological conversion of selenite remains a central theme in selenium oxyanion metabolism because selenite is commonly employed as a nutritional supplement in bacterial and mammalian cell cultures. The reduction of selenite in bacteria is related to at least three processes: assimilative reduction for incorporating selenium into cellular components, such as Sec in selenoproteins or selenouridine in tRNAs; dissimilative reduction in respiration; and detoxification [8]. In various bacterial species, diverse redox molecules and enzymes, such as glutathione [14, 15], thioredoxin [16], fumarate reductase [17], nitrate reductase [18], nitrite reductase [19, 20], and sulfite reductase [21], have been identified as participants in the reduction of selenite.

In the extensively investigated bacterium *Escherichia coli* K-12, the reduction of selenite to selenide is postulated to occur within the cytoplasm. This selenide is then utilized in the assimilation pathway for the synthesis of the selenoprotein formate dehydrogenase (FDH) [22]. Conversely, excess selenide is converted into elemental selenium (Se^0) and accumulates as extracellular SeNPs in the detoxification pathway [23, 24]. The reduction of selenite in *E. coli* is hypothesized to be facilitated by two major redox systems: the thioredoxin (Trx) system and the glutathione (GSH) system [14]. The Trx system comprises thioredoxin 1 (Trx1) encoded by the *trxA* gene, thioredoxin reductase encoded by *trxB*, and NADPH [25]. Trx1 is a small, ubiquitous protein with two conserved cysteine residues that catalyze numerous redox reactions through the reversible oxidation of its active site dithiol to a disulfide. Oxidized thioredoxin is subsequently be reduced by the flavoenzyme thioredoxin reductase with NADPH. *E. coli* has an additional thioredoxin variant, thioredoxin 2 (Trx2), which is encoded by the *trxC* gene and characterized by an extended N-terminus and thermosensitivity [26]. The Trx system is present in all bacteria and functions in a wide variety of cellular processes [25, 27]. In contrast, the GSH system consists of GSH produced by GSH synthase, encoded by the *gshB* gene, GSH reductase, encoded by the *gor* gene, and NADPH [28]. GSH is the major low-molecular-weight thiol in *E. coli*, and it protects cells not only as an antioxidant, but also as a detoxifying molecule against reactive species and electrophiles. Oxidized GSH is reduced by GSH reductase with NADPH. Although GSH is abundant in many organisms and serves as a prominent thiol and antioxidant, it is scarce in most Gram-positive bacteria [29]. However, the extent to which these reducing systems are involved in the assimilation and detoxification-reduction pathways of selenite is not well understood. In this study, we investigated the effects of single-gene deletions in the Trx or GSH system of *E. coli* on SeNP formation, selenite sensitivity, and selenoprotein biosynthesis.

Materials and methods

Bacterial strains and culture conditions

E. coli K-12 BW25113 (a wild-type strain) and its single-gene mutant strains JW585-KC6 (Δ*trxA*), JW0871-KC (Δ*trxB*), JW2566-KC (Δ*trxC*), JW2914-KC (Δ*gshB*), and JW3467-KC (Δ*gor*) were obtained from the National BioResource Project (National Institute of Genetics, Japan). *E. coli* cells were pre-cultured overnight at 37°C in Luria–Bertani (LB) medium (5 g/L yeast extract, 10 g/L tryptone, and 10 g/L sodium chloride) and then inoculated at an optical density at 600 nm (OD_{600}) = 0.01 into 5 mL of tryptic soy broth (TSB) medium (17 g/L pancreatic digest of casein, 3 g/L papaic digest of soybean, 2.5 g/L dextrose, 5 g/L sodium chloride, 2.5 g/L dipotassium phosphate) containing various concentrations of sodium selenite, followed by culturing at 37°C under aerobic conditions with shaking at 220 rpm. Kanamycin was added at a concentration of 50 mg/L to the pre-culture of the mutant strains.

Bacterial growth measurement

After 6, 24, and 48 h of culture under the conditions described above, the pellets containing bacterial cells and SeNPs were collected by centrifugation at 11,000 × *g* for 2 min. To remove SeNPs outside of bacterial cells, the pellets were treated with 100 mM DTT in 20 mM phosphate-buffered saline PBS (pH 7.5). The OD_{600} of bacterial cells was measured after the red color due to SeNPs disappeared.

Determination of selenite by hydride generation-atomic fluorescence spectrometry

Selenite in the bacterial culture supernatant was determined using a hydride-generation atomic fluorescence spectrometer (HG-AFS) (Millennium Excalibur, PSA, Orpington, UK) equipped with a selenium PS analytical lamp (P849SF Photoron Pty Ltd., Victoria, Australia), as previously described [30], after centrifugation of the culture supernatant sample at 15,000 × *g* for 15 min. The analytical conditions for HG-AFS were as follows: injection volume, 100 µL; acid carrier, 0.5% (w/v) KBr in 6 M

HCl; and reductant, 0.7% (w/v) $NaBH_4$ in 0.1 M NaOH.

Quantification and statistical analysis

All quantification experiments were performed in three replicates and the results are shown as mean ± standard deviation (SD). An unpaired *t*-test (Student's *t* test) is appropriate and was used for such comparisons. Dunnett test was applied to experiments with three or more groups. The statistical significance of differences between experimental groups was determined with R software. A *P* value of less than 0.01 was considered statistically significant.

Selenite sensitivity assay

E. coli cells were streaked onto TSB agar plates containing 0, 1, 5, 10, or 20 mM sodium selenite and incubated at 37°C for 48 h.

FDH assay on a solid agar medium

FDH was assayed using the benzyl viologen agar overlay method [31]. *E. coli* cells were anaerobically cultured overnight on solid LB medium containing 0.5% glucose at 37°C. The medium was then overlaid with 0.75% agar containing 1.0 mg mL^{-1} benzyl viologen, 3.4 mg mL^{-1} KH_2PO_4, and 17 mg mL^{-1} sodium formate.

Results and discussion

Effects of mutations in the Trx and GSH systems on SeNPs formation via selenite reduction

To assess the involvement of the Trx and GSH systems in selenite reduction, *E. coli* strains with deletions in thioredoxin-related genes (*trxA*, *trxB*, and *trxC*) or GSH-related genes (*gshB* and *gor*) were cultured in the presence or absence of 1 mM selenite. This selenite concentration was employed according to the previous studies [24, 32]. The reduction of selenite was assayed based on the development of a red color, attributed to the excitation of surface plasmon vibrations in the resulting SeNPs. As shown in **Figure 1**, all of the strains reduced selenite to produce a red color (i.e., SeNPs) after 24-h cultivation. On the other hand, the growth of each bacterial strain was significantly inhibited by the addition of 1 mM selenite, in contrast to growth in the absence of selenite (**Figure 2 (a)**). In all strains except Δ*gshB*, more than 96% of the selenite was removed from the medium at 24 h, while for the Δ*gshB* strain, the reduction was 66% at 24 h but reached 99% at 48 h (**Figure 2 (b)**). The selenite reduction efficiency, defined as the reduced selenite concentration normalized by the number of cells (OD_{600}), of Δ*gshB* at 24 h was slightly but significantly lower than that of the wild-type (WT) strain (**Figure 2 (c)**). Nevertheless, all strains were able to almost completely reduce selenite after 48 h (**Figure 2 (b)**). These results show that disruption of a single gene in either the Trx or GSH system did not drastically affect SeNP formation via selenite reduction by *E. coli* in the presence of 1 mM selenite.

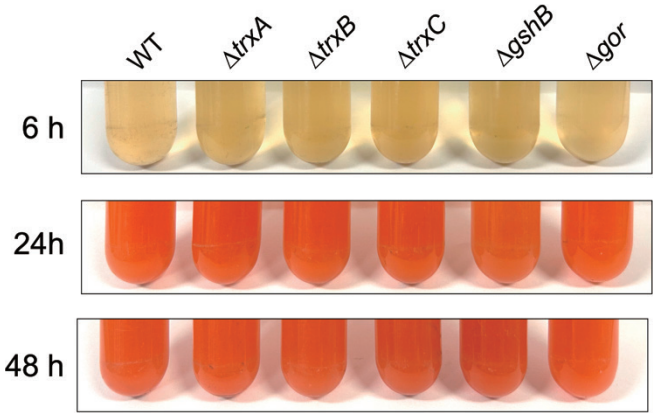

Figure 1. SeNP formation by the *E. coli* strains
Formation of red-colored SeNPs via selenite reduction by the WT and mutant strains of *E. coli*. The cells were cultured at 37°C in TSB medium containing 1 mM selenite.

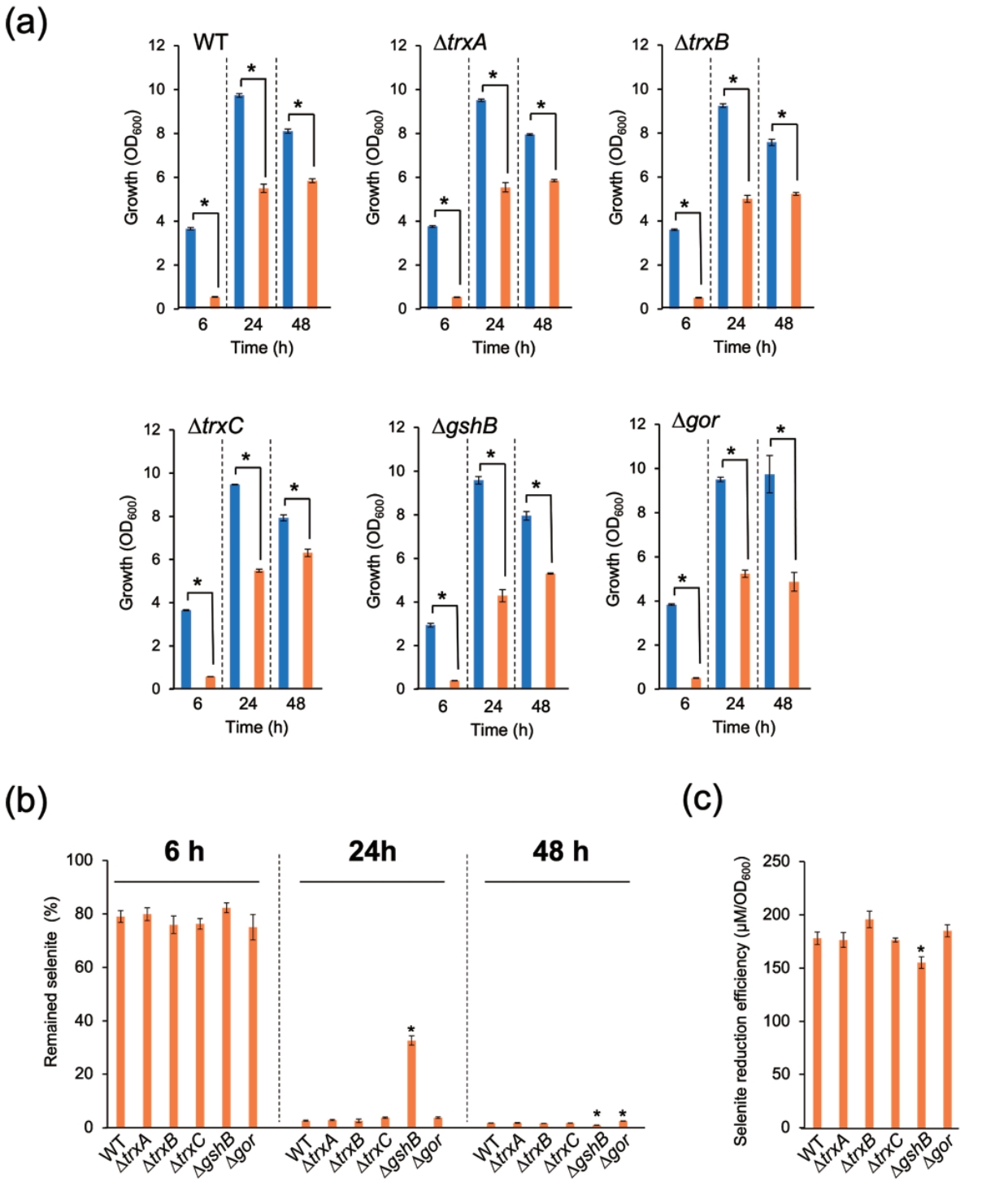

Figure 2. **Growth and selenite reduction ability of the *E. coli* strains**

(a) Growth (OD_{600}) of the WT and mutant strains cultured at 37°C in TSB medium with (orange) or without (blue) 1 mM selenite for 6 h, 24 h, and 48 h. The data are expressed as means ± SD (n = 3). Statistical analysis was performed by the t-test. *, $P < 0.01$ compared with WT.

(b) Amount of remained selenite in the culture supernatant of WT and mutant strains cultured at 37°C in TSB medium containing 1 mM sodium selenite for 6 h, 24 h, and 48 h. The data are expressed as means ± SD (n = 3). Statistical analysis was performed by the Dunnett test. *, $P < 0.01$ compared with WT.

(c) The selenite reduction efficiency, defined as the reduced selenite concentration normalized by the number of *E. coli* cells (OD_{600}) cultured at 37°C in TSB medium containing 1 mM sodium selenite for 24 h. The concentration of reduced selenite was calculated by subtracting the remained selenite concentration in the culture supernatant at 24 h from the initial selenite concentration at 0 h (1 mM). The data are expressed as means ± SD (n = 3). Statistical analysis was performed by the Dunnett test. *, $P < 0.01$ compared with WT.

Effect of mutations in the Trx and GSH systems on selenite sensitivity

To examine whether mutations in the Trx and GSH systems affect the sensitivity of *E. coli* to higher levels of selenite, WT and mutant strains were cultured on TSB agar medium containing 0, 1, 5, 10, or 20 mM selenite. All mutant strains grew similarly to the WT strain in the absence of selenite. However, marked growth inhibition was observed for the Δ*trxB*, Δ*gshB*, and Δ*gor* strains at 5–20 mM selenite compared with the WT (**Figure 3**), suggesting increased selenite sensitivity in these mutant strains. In contrast, deletion of *trxA* or *trxC* resulted in no drastic change in selenite sensitivity at 5–20 mM selenite compared with the WT. These results suggest that *trxB*, *gshB*, and *gor* are important for bacterial tolerance to > 5 mM selenite.

GSH is known to react with selenite to produce selenodiglutathione (GS-Se-SG) [14, 33]. The reduction of GS-Se-SG by GSH, thioredoxin, GSH reductase, or thioredoxin reductase is thought to form GSH selenopersulfide (GS-SeH), which is ultimately reduced to GSH and Se^0 [34-36]. Kessi and Hanselmann suggested that the same type of reaction is involved in the formation of SeNPs in *Rhodospirillum rubrum* and *E. coli* [15]. Our results are consistent with the previous observations and highlight the importance of thioredoxin reductase, GSH synthase, and GSH reductase in conferring selenite tolerance linked to SeNP synthesis via selenite reduction. The small effects of the deletion of either *trxA* or *trxC* on selenite tolerance and selenite reduction were probably due to the redundant functions of these thioredoxins.

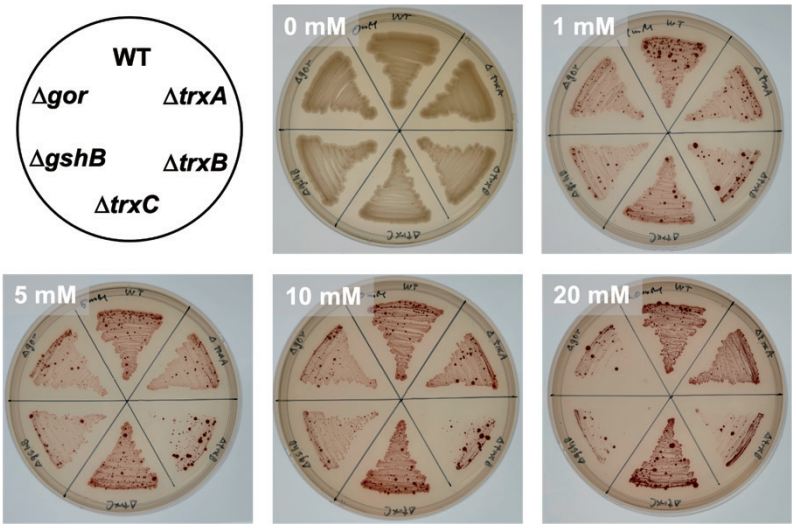

Figure 3. Selenite sensitivity of the *E. coli* strains
The WT and mutant strains of *E. coli* were streaked on TSB agar plates containing 0, 1, 5, 10, or 20 mM selenite. All plates were incubated at 37°C for 48 h.

Involvement of the Trx system in selenoprotein synthesis

To investigate whether the Trx and GSH systems are involved in selenoprotein biosynthesis, the activity of the selenoprotein FDH was assayed in whole *E. coli* cells anaerobically cultured on solid medium using benzyl viologen, as previously described [16]. **Figure 4** shows that WT cells were stained purple, indicating FDH activity. In contrast, Δ*trxA* cells were not stained in the assay, indicating a loss of FDH activity. Similarly, Δ*trxB* cells had slightly lower FDH activity than WT. In contrast, the loss of *trxC*, *gshB*, or *gor* had no effect on the FDH activity, which was comparable to that of the WT cells. These results suggest that the Trx system is important for selenite utilization during selenoprotein biosynthesis. Our results agree well with those of previous studies by Shimizu *et al.* [16] and Takahata *et al*. [22], which also suggest involvement of the Trx system in the selenium assimilation pathway. Interestingly, our results show that TrxC could not replace TrxA in selenoprotein biosynthesis, whereas these thioredoxins can be replaceable during SeNP synthesis. This suggests that there are at least two different pathways for

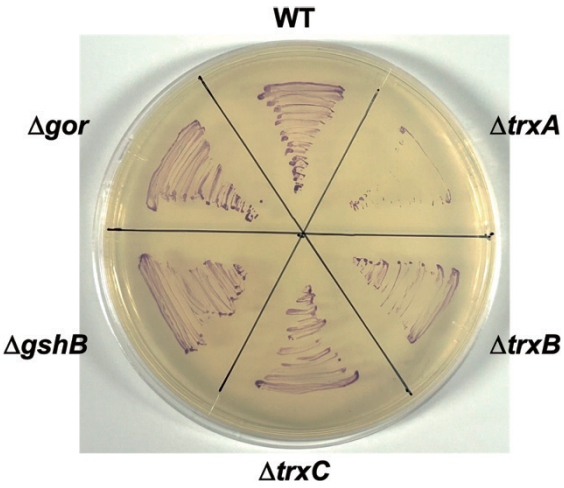

Figure 4. Whole-cell FDH assay of the *E. coli* strains
The WT and mutant strains of *E. coli* were anaerobically cultured at 37°C for 18 h on LB agar plate containing 0.5% glucose, followed by FDH assay using benzyl viologen.

selenite reduction in *E. coli*: a specific selenite assimilation (i.e., selenoprotein biosynthesis) pathway by the Trx system and a non-specific detoxification (i.e., SeNP synthesis) pathway involving both of the GSH and Trx systems.

Acknowledgments

This study was supported by KAKENHI grants from the JSPS (20J40237 to A.O., 20H02907 and 22H04823 to H.M.), the Ritsumeikan Global Innovation Research Organization, the Program for the Third-Phase R-GIRO Research (to H.M.), and the Analysis and Development System for Advanced Materials (ADAM) of RISH, Kyoto University, as a collaborative program.

References

[1] Hatfield DL, Tsuji PA, Carlson BA, Gladyshev VN: Selenium and selenocysteine: roles in cancer, health, and development. *Trends Biochem Sci*. 2014; 39: 112-120.

[2] Rayman MP: Selenium and human health. *Lancet*. 2012; 379: 1256-1268.

[3] Schomburg L: Selenium deficiency due to diet, pregnancy, severe illness, or COVID-19-A preventable trigger for autoimmune disease. *Int J Mol Sci*. 2021; 22: 8532.

[4] Böck A, Forchhammer K, Heider J, Leinfelder W, Sawers G, Veprek B, Zinoni F: Selenocysteine: the 21st amino acid. *Mol Microbiol*. 1991; 5: 515-520.

[5] Zhang Y, Gladyshev VN: An algorithm for identification of bacterial selenocysteine insertion sequence elements and selenoprotein genes. *Bioinformatics*. 2005; 21: 2580-2589.

[6] Kryukov GV, Castellano S, Novoselov SV, Lobanov AV, Zehtab O, Guigo R, Gladyshev VN: Characterization of mammalian selenoproteomes. *Science*. 2003; 300: 1439-1443.

[7] Rayman MP: The importance of selenium to human health. *Lancet*. 2000; 356: 233-241.

[8] Staicu LC, Oremland RS, Tobe R, Mihara H: Bacteria versus selenium: A vew from the inside out. *Selenium in plants.* (ed by Pilon-Smits E, Winkel L, Lin Z): Springer; 2017, 79-108.

[9] Oremland RS, Herbel MJ, Blum JS, Langley S, Beveridge TJ, Ajayan PM, Sutto T, Ellis AV, Curran S: Structural and spectral features of selenium nanospheres produced by Se-respiring bacteria. *Appl Environ Microbiol*. 2004; 70: 52-60.

[10] Rech SA, Macy JM: The terminal reductases for selenate and nitrate respiration in *Thauera selenatis* are two distinct enzymes. *J Bacteriol*. 1992; 174: 7316-7320.

[11] Kuroda M, Notaguchi E, Sato A, Yoshioka M, Hasegawa A, Kagami T, Narita T, Yamashita M, Sei K, Soda S, Ike M: Characterization of *Pseudomonas stutzeri* NT-I capable of removing soluble selenium from the aqueous phase under aerobic conditions. *J Biosci Bioeng*. 2011; 112: 259-264.

[12] Kagami T, Narita T, Kuroda M, Notaguchi E, Yamashita M, Sei K, Soda S, Ike M: Effective selenium volatilization under aerobic conditions and recovery from the aqueous phase by *Pseudomonas stutzeri* NT-I. *Water Res*. 2013; 47: 1361-1368.

[13] Chasteen TG, Bentley R: Biomethylation of selenium and tellurium microorganisms and plants. *Chem Rev*. 2002; 103: 1-25.

[14] Turner RJ, Weiner JH, Taylor DE: Selenium metabolism in *Escherichia coli*. *BioMetals*. 1998; 11: 223-227.

[15] Kessi J, Hanselmann KW: Similarities between the abiotic reduction of selenite with glutathione and the dissimilatory reaction mediated by *Rhodospirillum rubrum* and *Escherichia coli*. *J Biol Chem*. 2004; 279: 50662-50669.

[16] Shimizu A, Tobe R, Aono R, Inoue M, Hagita S, Kiriyama K, Toyotake Y, Ogawa T, Kurihara T, Goto K, Prakash NT, Mihara H: Initial step of selenite reduction via thioredoxin for bacterial selenoprotein biosynthesis. *Int J Mol Sci*. 2021; 22: 10965-10975.

[17] Wells M, McGarry J, Gaye MM, Basu P, Oremland RS, Stolz JF: Respiratory selenite reductase from *Bacillus selenitireducens* strain MLS10. *J Bacteriol*. 2019; 201: e00614-e00618.

[18] Sabaty M, Avazeri C, Pignol D, Vermeglio A: Characterization of the reduction of selenate and tellurite by nitrate reductases. *Appl Environ Microbiol*. 2001; 67: 5122-5126.

[19] Basaglia M, Toffanin A, Baldan E, Bottegal M, Shapleigh JP, Casella S: Selenite-reducing capacity of the copper-containing nitrite reductase of *Rhizobium sullae*. *FEMS Microbiol Lett*. 2007; 269: 124-130.

[20] DeMoll-Decker H, Macy JM: The periplasmic nitrite reductase of *Thauera selenatis* may catalyze the reduction of selenite to elemental selenium. *Arch Microbiol*. 1993; 160: 241-247.

[21] Harrison G, Curle C, Laishley EJ: Purification and characterization of an inducible dissimilatory type sulfite reductase from *Clostridium pasteurianum*. *Arch Microbiol*. 1984; 138: 72-78.

[22] Takahata M, Tamura T, Abe K, Mihara H, Kurokawa S, Yamamoto Y, Nakano R, Esaki N, Inagaki K: Selenite assimilation into formate dehydrogenase H depends on thioredoxin reductase in *Escherichia coli*. *J Biochem*. 2008; 143: 467-473.

[23] Gerrard TL, Telford JN, Williams HH: Detection of selenium deposits in *Escherichia coli* by electron microscopy. *J Bacteriol*. 1974; 119: 1057-1060.

[24] Zhu TT, Tian LJ, Yu HQ: Phosphate-suppressed selenite biotransformation by *Escherichia coli*. *Environ Sci Technol*. 2020; 54: 10713-10721.

[25] Holmgren A: Thioredoxin. *Annu Rev Biochem*. 1985; 54: 237-271.

[26] Miranda-Vizuete A, Damdimopoulos AE, Gustafsson J, Spyrou G: Cloning, expression, and characterization of a novel *Escherichia coli* thioredoxin. *J Biol Chem*. 1997; 272: 30841-30847.

[27] Potamitou A, Holmgren A, Vlamis-Gardikas A: Protein levels of *Escherichia coli* thioredoxins and glutaredoxins and their relation to null mutants, growth phase, and function. *J Biol Chem*. 2002; 277: 18561-18567.

[28] Faulkner MJ, Veeravalli K, Gon S, Georgiou G, Beckwith J: Functional plasticity of a peroxidase allows evolution of diverse disulfide-reducing pathways. *Proc Natl Acad Sci U S A*. 2008; 105: 6735-6740.

[29] Fahey RC, Brown WC, Adams WB, Worsham MB: Occurrence of glutathione in bacteria. *J Bacteriol*. 1978; 133: 1126-1129.

[30] Sanchez-Rodas D, Mellano F, Morales E, Giraldez I: A simplified method for inorganic selenium and selenoaminoacids speciation based on HPLC-TR-HG-AFS. *Talanta*. 2013; 106: 298-304.

[31] Mandrand-Berthelot M-A, Wee MYK, Haddock BA: An improved method for the identification and characterization of mutants of *Escherichia coli* deficient in formate dehydrogenase activity. *FEMS Microbiol Lett*. 1978; 4: 37-40.

[32] Kora AJ, Rastogi L: Bacteriogenic synthesis of selenium nanoparticles by *Escherichia coli* ATCC 35218 and its structural characterisation. *IET Nanobiotechnol*. 2017; 11: 179-184.

[33] Hsieh HS, Ganther HE: Acid-volatile selenium formation catalyzed by glutathione reductase. *Biochemistry*. 1975; 14: 1632-1636.

[34] Ganther HE: Reduction of the selenotrisulfide derivative of glutathione to a persulfide analog by glutathione reductase. *Biochemistry*. 1971; 10: 4089-4098.

[35] Ganther HE: Selenotrisulfides. Formation by the reaction of thiols with selenious acid. *Biochemistry*. 1968; 7: 2898-2905.

[36] Sandholm M, Sipponen P: Formation of unstable selenite-glutathione complexes in vitro. *Arch Biochem Biophys*. 1973; 155: 120-124.